

Polyisocyanate-based water-soluble polyurethane/CaCO₃ composites for gunpowder storage



Eyob Wondu ^a, Zelalem Chernet Lule ^b, Jooheon Kim ^{a,*}

^a Graduate School of Intelligence Energy and Industry, Chung-Ang University, Seoul, 156-756, South Korea

^b School of Chemical Engineering and Material Science, Chung-Ang University, Seoul, 156-756, South Korea

ARTICLE INFO

Keywords:

Polyisocyanate
Water-soluble polyurethane
Mechanical property
Thermal stability
Solution polymerization

ABSTRACT

The need for improved gunpowder storage to recycle used gunpowder is increasing due to global warming and the economic losses incurred by withdrawing the gunpowder and by its storage. Herein, we fabricated an aliphatic water-soluble polyurethane (WPU) to be used for gunpowder storage, which allows for easy separation of the matrix (WPU) from the gunpowder by solubilizing the WPU with water. We used an aliphatic polyisocyanate as the main hard segment and polyethylene glycol as the soft segment. The usage of an aliphatic polyisocyanate is assumed to enhance the thermal stability and mechanical properties of the composites. We applied the solution polymerization process to fabricate the WPU. CaCO₃ was used as a fake gunpowder. The tensile strength of the 40% diisocyanate-treated CaCO₃ WPU composites was increased by 3.5 times as compared to the neat WPU and the elongation at break point was also significantly improved. The thermal stability of the composites was greatly improved by the utilization of the treated CaCO₃ particles in the WPU matrix. The hydrophilic nature, identified by contact angle measurements, of the composite is interesting, less than 65°, which proves a good hydrophilic composite has been fabricated. The structure of the polymer was confirmed via FTIR analysis and proton NMR investigation.

1. Introduction

Recently, the use of non-volatile organic compounds in order to reduce environmental pollution (a major concern of the United Nations [1]) has been suggested to prevent environmental disaster [2]. Among the volatile organic compounds, product storage materials are major contributors [3–8]. Replacing these storage materials is necessary to preserve the environment. Water-dispersible polymers are one of the candidates for the storage of gunpowder due to their high availability, low cost, and easy fabrication. Aliphatic water-soluble polyurethanes (WPU), water-dispersible polymers [2,5–14], are a good sustainable replacement for gunpowder storage as they have good thermal stability and mechanical properties.

Research on aliphatic polyisocyanates has shown promise for improving mechanical properties, increasing flame retardancy [15,16], and developing two-packed polyurethanes [8,15]. Research on water-soluble polyurethanes using polyisocyanates as the main component of the hard segment is still in progress [8,15,17–19].

Gao et al. [9] prepared a well-dispersed water-soluble polyurethanes composites made up from a water-borne polyurethane and nano

particles of CaCO₃. They studied the composites after modifying the surface of CaCO₃ particles with the help of oleic acid (OA). Their finding said that improvement of CaCO₃ using OA has increased the thermal stability. In our previous work [10], we fabricated thermally stable water-soluble polyurethane composites, filled with various loading of CaCO₃, with a potential to be used as a gunpowder storage. We demonstrated the thermo-mechanical properties of the fabricated composites to be applied in the gunpowder storages.

Water-soluble polyurethanes are polyurethanes that are water-dispersible due to the introduction of emulsifiers into the polymer chain which make the final polymer ionized. They are produced with the help of both aliphatic and aromatic diisocyanates; aliphatic diisocyanates are UV-radiation resistive, while aromatic diisocyanates are attacked by UV-radiation [20]. There are different ways of manufacturing WPUs, including solution processes [8–10,13,14,21–24], prepolymer mixing processes [3,12,22,25–28], ketamine-ketazine processes [12,29], and melt-mixing [12,13,22,30].

In this work, we fabricated an aliphatic WPU from an aliphatic polyisocyanate as the main hard segment and polyethylene glycol as the soft segment chain of the WPU. Polyisocyanates were used to improve

* Corresponding author.

E-mail address: jooheonkim@cau.ac.kr (J. Kim).

the sticky nature and poor mechanical properties of the diisocyanate main hard segment based WPUs. Solution polymerization was applied to fabricate the WPU under a nitrogen gas atmosphere. The structural, mechanical, thermal, hydrophilic, and morphological properties were characterized by Fourier transform infrared spectroscopy, proton nuclear magnetic resonance spectroscopy, Universal testing machine, Dynamic mechanical analysis, thermogravimetric analysis, contact angle measurements and FE-SEM analysis. The thermal degradation and mechanical properties (tensile strength, elongation at break, and modulus) were improved by the use of polyisocyanates as hard segments. In addition, applying isophorone diisocyanate (IPDI)-treated CaCO_3 particles, using CaCO_3 as fake gunpowder, significantly further enhanced those properties.

2. Materials and methods

2.1. Materials

Calcium carbonate (CaCO_3 , 99%) was generously provided by The South Korea Agency for Defense Development (ADD). Dae-Jung Chemical and Metal Co. Ltd. (Seoul, Korea) provided acetone, polyethylene glycol (PEG, $M_w = 4000$), and sodium hydroxide (NaOH , >94%). Isophorone diisocyanate (IPDI, 98%), dimethylolpropionic acid (DMPA, 98%), dibutyltin dilaurate (DBTDL, 99%), 1,4-butanediol (BD, 99%) were purchased from Sigma-Aldrich (St. Louis, MO, USA). Aliphatic polyisocyanate (PI) was kindly provided by BASF (Ludwigshafen, Germany), and Alfa Aesar provided the neutralizer, triethylamine (TEA, >99%). All the raw materials were used as-is without further modification.

3. Methods

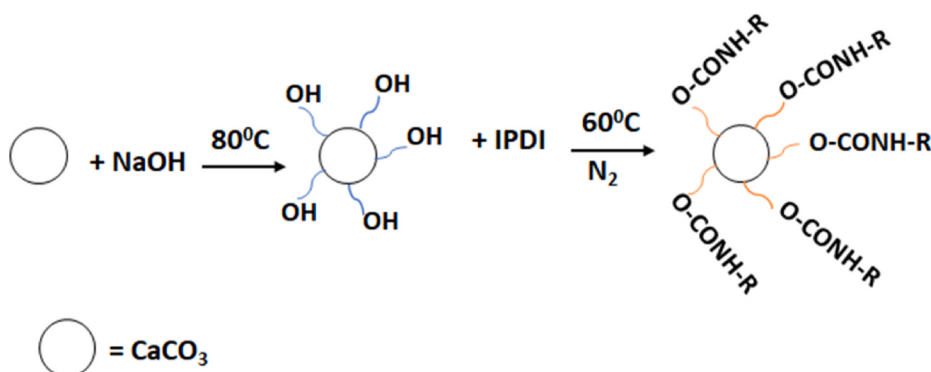
The CaCO_3 particle surfaces were treated with isophorone diisocyanate (IPDI). The surface treatment of CaCO_3 particles with IPDI was performed as follows. Initially, the CaCO_3 particles were dried in an oven for 24 h at 80 °C to remove moisture and impurities. The dried CaCO_3 particles were hydroxylated (OH-treated) with 100 mL of 3 M NaOH solution. Then, the solution was mixed for approximately 24 h at 80 °C. The OH-treated CaCO_3 particles were then neutralized with deionized water by washing with vacuum filtration. The neutralized filter cake was then dried at 60 °C for 24 h. The oven-dried, OH-treated CaCO_3 particles were then dissolved in acetone and immersed in an oil bath at a temperature of 60 °C in a three-necked round-bottom flask with a condenser, nitrogen inlet, and stirrer. Then, 5 wt% of IPDI was added to the solution, which was mixed for 6 h after simultaneous addition of the DBTDL catalyst. Finally, the diisocyanate-treated CaCO_3 particles were filtered to separate the solvent from the particles and dried at 60 °C for 24 h to remove any remaining acetone. The surface treatment of CaCO_3 with IPDI was dictated in Scheme 1.

The water-soluble polyurethane based on polyisocyanate was produced using the acetone process. Acetone was used as a solvent to regulate the viscosity during the course of the reaction. Initially, an appropriate amount of IPDI-treated CaCO_3 particles were mixed with the PEG in acetone for 2 h at 60 °C. Following the mixing of IPDI-treated CaCO_3 particles with PEG, an emulsifier (DMPA) was added. After dissolving the DMPA, polyisocyanate (PI) was added to the reaction at a ratio of 1:3 with respect to PEG. The reaction occurred in a round-bottomed, three-necked flask with a dropping funnel, mechanical stirrer, and condenser in an oil bath under a nitrogen gas atmosphere. The reaction mixture was left to react for about 4 h at 80 °C. When an increase in viscosity was observed, an acetone was added to control it, and then the chain extender (BD) was added to the system at a ratio of 1:1 with respect to the polyol (PEG). The chain extension process was carried out for 2 h. Then, the neutralization process was carried out upon completion of chain extension with the help of TEA to neutralize the carboxyl groups arising from DMPA after reducing the temperature to 50 °C. Finally, the product was separated from the flask and put on a Petri dish to be cured. The curing was carried out for 24 h in air, followed by vacuum drying at 40 °C for 24 h. Finally, the product was molded into the required shape for further analysis. The samples were prepared such that there were 10 step sizes in the production stages. From here on, we have denoted all the specimens fabricated as neat-WPU, 10-TWPU, 20-TWPU, 30-TWPU, 40-TWPU, and 40WPU to replace the neat water-soluble polyurethane, 10%, 20%, 30%, 40% IPDI treated CaCO_3 - water-soluble polyurethane, and 40% pristine CaCO_3 -water-soluble polyurethane respectively.

3.1. Characterization

Both the surface treatment of the CaCO_3 particles and the structural analysis of the WPU were evaluated via Fourier transform infrared spectroscopy (FTIR; Nicolet, iS5, Thermo Fisher Scientific, Seoul, Korea). The chemical structure of the WPU was further confirmed by proton nuclear magnetic resonance (^1H NMR 300 Hz, Gemini 2000, Varian, Palo Alto, CA, USA). The amount of IPDI attached to the CaCO_3 particles was determined by thermogravimetric analysis (TGA-2050, TA Instruments, New Castle, DE, USA) and field emission scanning electron microscopy (FE-SEM; Sigma, Carl Zeiss, Oberkochen, Germany) was used to evaluate the adhesion of the IPDI to the CaCO_3 particles. The elemental composition of pristine and IPDI-treated CaCO_3 particles was evaluated by X-ray photoelectron spectroscopy (XPS; K-Alpha, Thermo Fisher Scientific). The XPS measurements were taken from the background of Al $K\alpha$ monochromatic. Gaussian fitting was used to fit the curves of all the deconvoluted results keeping the spectrum width constant.

A drop shape analyzer (DSA100, KRÜSS GmbH, Hamburg, Germany) was used to evaluate the hydrophilic nature of the neat WPU and the IPDI-treated, CaCO_3 -based WPU composites. The measurement was



Scheme 1. Hydroxyl attachment and IPDI treatment of CaCO_3 particles.

taken using a 5 μL water droplet on a flat sample at room temperature. TGA was used to evaluate the thermal stability of the neat WPU and the IPDI-treated CaCO_3 -based WPU composites at a heating rate of 20 $^{\circ}\text{C}/\text{min}$ under a nitrogen atmosphere at a temperature range of 30–600 $^{\circ}\text{C}$. The melting properties of the neat WPU and the IPDI-treated CaCO_3 -based WPU composites were evaluated by means of differential scanning calorimetry (DSC, DSC-7, PerkinElmer Co., Mougins, France). The morphology of the CaCO_3 particles and WPU were evaluated by means of a field emission scanning electron microscopy after fracturing the specimens with liquid nitrogen and coating the specimens with platinum to inhibit the movement of electrons which cause charging during the spectroscopic analysis.

The tensile properties of the neat WPU and both the untreated and the IPDI-treated CaCO_3 -based WPU composites were evaluated by means of a universal testing machine (UTM; model UTM-3344, Instron, Norwood, MA, USA) at a load rate of 10 mm/min with a maximum load of 2 KN. The viscoelastic properties (storage modulus and relaxation) of the neat WPU and both the untreated and the IPDI-treated CaCO_3 -based WPU composites were evaluated by means of the dynamic mechanical analysis (DMA; Triton Tech., London, UK) at a temperature range of -60–65 $^{\circ}\text{C}$ with a heating rate of 10 $^{\circ}\text{C}/\text{min}$ using liquid nitrogen for cooling.

4. Results and discussions

In this work, we sought to study the effects of CaCO_3 particles on the PI-based WPUs as well as the effects of using PI as a diisocyanate group to modify the thermal and mechanical properties of the final polymer. For this purpose, we fabricated various specimens using the solution process. Treatment of the surface of CaCO_3 particles with diisocyanate (IPDI) is believed to enhance the interfacial interactions between the CaCO_3 particles and WPU. In addition, the use of IPDI will enhance the compatibility between the PEG and PI and thus promote the formation of WPU as the IPDI acts as a plasticizer. The fabricated composite was characterized using FTIR to confirm the structure of the urethane groups and the interfacial interactions and morphology were studied using FE-SEM. The tensile and viscoelastic properties were determined by UTM and DMA analysis, respectively. The thermal properties and hydrophilic characteristics were determined using TGA, DSC and contact angle measurements, respectively. **Scheme 2**, displays the fabrication technique of the IPDI treated CaCO_3 -Polyisocyanate based WPU.

The surface treatment of CaCO_3 particles was characterized by FTIR, XPS, FE-SEM, and TGA. We used FTIR analysis to confirm the attachment of NCO groups to the CaCO_3 particles arising from the diisocyanate groups of IPDI. Infrared spectroscopy was used to compare the pristine CaCO_3 particles to the hydroxyl-modified IPDI-treated particles. The hydroxyl group attachment was confirmed by the appearance of OH-group peaks around 3300 cm^{-1} . The carbonyl stretching peaks appeared at 1235 cm^{-1} due to the interactions of NCO groups with the OH groups. The sharp peaks around 2950 and 2870 cm^{-1} are associated with methylene groups, whereas the NCO attachment to the OH-treated CaCO_3 particles is observed around 2250 cm^{-1} , which confirms the surface treatment was done perfectly. Further, the IPDI treatment was further confirmed by the appearance of NH- peaks around 3320 cm^{-1} and the NH-stretching at a wavenumber of around 1660 cm^{-1} . The

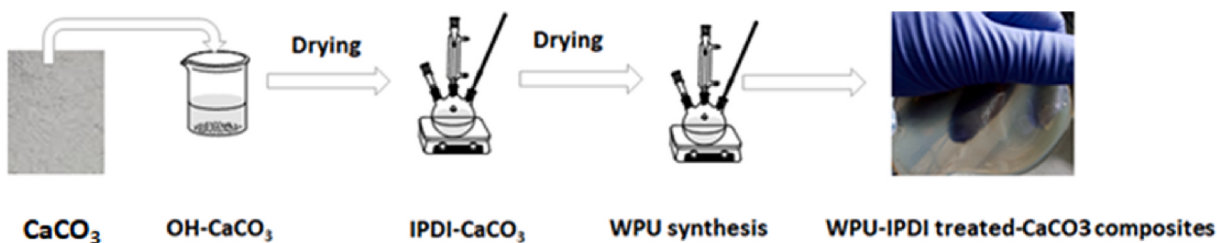
appearance of NH-, C=O, NCO, and CH_2 peaks confirms the surface treatment of CaCO_3 particles was successful. The results of the FTIR analysis are shown in **Fig. 1** (a).

To further confirm the surface treatment of CaCO_3 particles quantitatively, XPS analysis (elemental composition analysis) was used to confirm the appearance of N1s. The XPS analysis was used to identify the differences between the elemental composition of the IPDI-treated CaCO_3 particles and the pristine CaCO_3 particles. Both specimens to be analyzed were initially dried in an oven to remove impurities and moisture. **Fig. 1** (b) shows the wide survey scan of the pristine CaCO_3 and IPDI-treated CaCO_3 particles. The new peak appearing at a binding energy of around 401 eV corresponds to the N1s elements arising from the attachment of IPDI to the CaCO_3 particles. The intensity of the C1s, O1s increases with the treatment of IPDI as compared to the pristine CaCO_3 . The atomic percentages confirm the treatment of CaCO_3 particles with IPDI; for instance, the atomic percentage of C1s increases from 33.81% to 49.65%, respectively, for the pristine CaCO_3 and IPDI-treated CaCO_3 . Moreover, the intensity of N1s increases from 0.55 to 4.17 for the pristine and IPDI-treated CaCO_3 , respectively. The atomic percentage values of the specific elements are shown in **Table 1**. The attachment of IPDI to the CaCO_3 particles decreased the atomic percentage of Ca2p and O1s due to the incorporation of isocyanates onto the CaCO_3 particles.

Furthermore, the elemental decompositions were analyzed after deconvoluting the elemental photoelectron spectroscopy with Gaussian fitting methods. The results of the deconvolution analysis are shown in **Fig. 1(c-e)**. The N1s deconvolutions were performed between 394 and 406 eV; two deconvolutions peaks were obtained at 398 eV, which corresponds to C=N-C (amine groups), and at around 400 eV, which corresponds to C=O-N-C=O (amide groups).

The IPDI-treated CaCO_3 particles have only 1 O1s deconvoluted peak which corresponds to $\text{Ca}(\text{OH})_2$, whereas the pristine particles have 4 deconvolution peaks that correspond to impurities of which the main one is the $\text{Ca}(\text{OH})_2$. Moreover, the area covered by the deconvolution of O1s peaks decreases after the IPDI treatment because the diisocyanate group lacks oxygen. All of these data are displayed in **Table 1**. The area of both the C1s and N1s deconvolution peaks increased after the treatment of CaCO_3 particles with IPDI due to the attachment of amine and benzyl groups to the CaCO_3 particles, whereas the area of deconvolution peaks of O1s and Ca2p decreases after the treatment due to the lack of oxygen and calcium in the diisocyanate groups.

The attachment of IPDI to the CaCO_3 particles was also confirmed by TGA, which quantitatively determines the amount of IPDI attached to the particles in a similar manner to XPS. We treated the surface of CaCO_3 with 5 wt% of IPDI with respect to the weight of CaCO_3 treated. The TGA results shown in **Fig. 2** (a) demonstrate that the dried pristine CaCO_3 particles exhibit almost no degradation after being heated to 600 $^{\circ}\text{C}$, whereas the IPDI-treated CaCO_3 particles exhibit a degradation of about 4.78% which confirms the IPDI attachment to the CaCO_3 particles. The treatment of CaCO_3 particles was further analyzed using FE-SEM, as shown in **Fig. 2**. **Fig. 2** (b) shows the SEM monograph of pristine CaCO_3 particles, which shows many impurities on the surface in agreement with the XPS results. The FE-SEM images of the IPDI-treated CaCO_3 particles show pure particles (**Fig. 2** (c)). These analyses confirm that the treatment was successful.



Scheme 2. Synthesis route of IPDI treated CaCO_3 -Polyisocyanate based WPU.

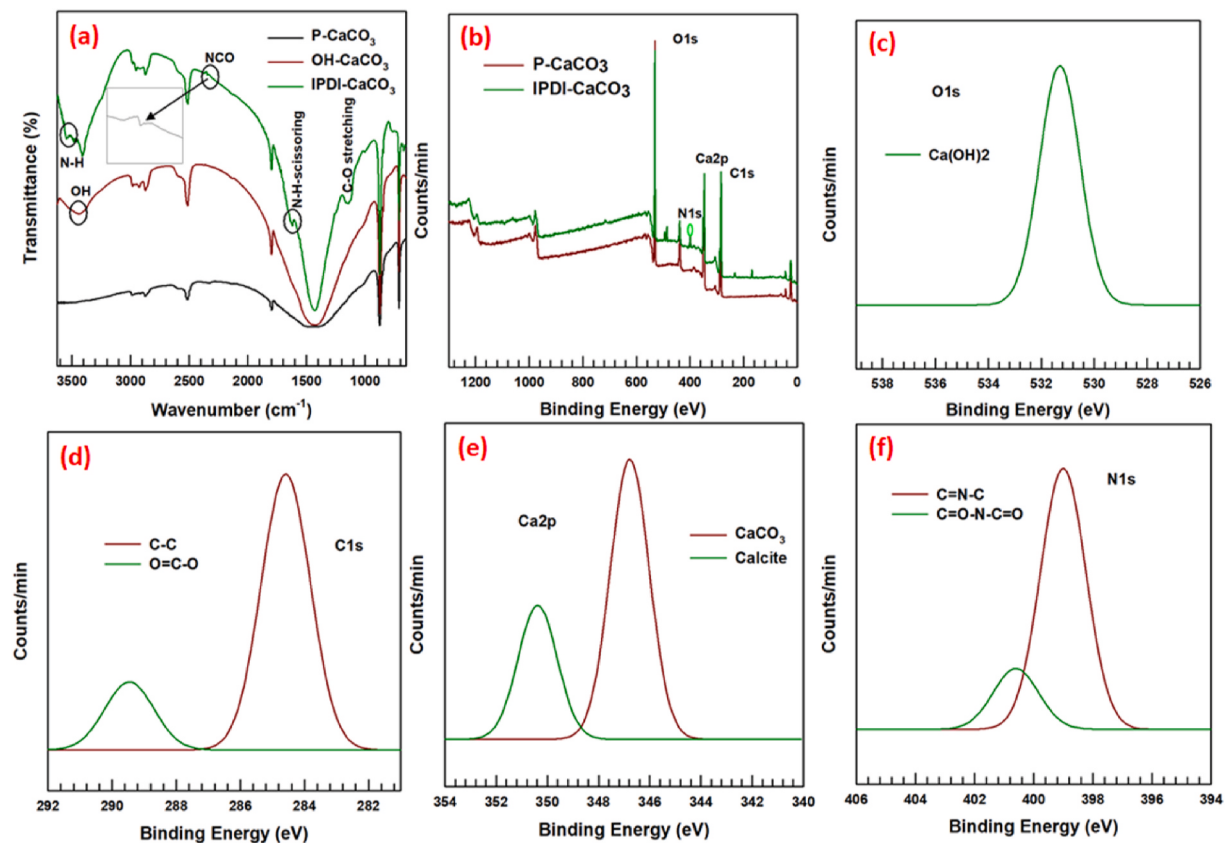


Fig. 1. Characterization of IPDI treated CaCO_3 particles: (a) FTIR analysis of the pristine and IPDI treated CaCO_3 particles; (b) XPS survey results of Pristine and IPDI treated CaCO_3 particles; (c), (d), (e), and (f) are the XPS deconvolution results of O1s, C1s, Ca2p, and N1s of IPDI treated CaCO_3 particles respectively.

Table 1
Elemental compositions of the pristine and IPDI- treated CaCO_3 particles.

Elements	Pristine CaCO_3 Atomic%	IPDI- treated CaCO_3 Atomic%	Area of deconvolution peaks of P- CaCO_3	Area of deconvolution peaks of IPDI treated- CaCO_3
O1s	49.4	35.82	149172.51	130734.13
C1s	33.81	49.65	41503.49	73676.24
Ca2p	16.24	10.35	97068.04	74784.48
N1s	0.55	4.17	1132.27	10327.45

The structure of the fabricated WPU was verified using FT-IR and NMR. The FTIR analysis was performed using the attenuated total reflectance method. The results are shown in Fig. 3 (a). The NH- peak at

a wavelength of $3300\text{--}3500\text{ cm}^{-1}$ appeared due to the formation of amine bonds in between the polyol and the polyisocyanate; moreover, this peak can also arise from the emulsifier neutralizing group, TEA. The methylene (CH_2) groups appeared around 2960 cm^{-1} . The peak around 1670 cm^{-1} was due to the carbonyl groups arising from the emulsifying group, DMPA, whereas the peak at 1470 cm^{-1} is associated with the O—C—O groups. The structure of the fabricated WPU was further confirmed using proton NMR with Dimethyl sulfoxide (DMSO) as the solvent and tetramethylsilane (TMS) as a background reference. The NMR analysis revealed a chemical shift around the 13 ppm corresponding to the OH groups arising from the polyol (PEG) and another one around 3 ppm corresponding to the NCO groups originating from the polyisocyanate groups. The appearance of both the OH and NCO groups on the chemical shift confirms the formation of the WPU. The output of the NMR analysis is shown in Fig. 3 (b).

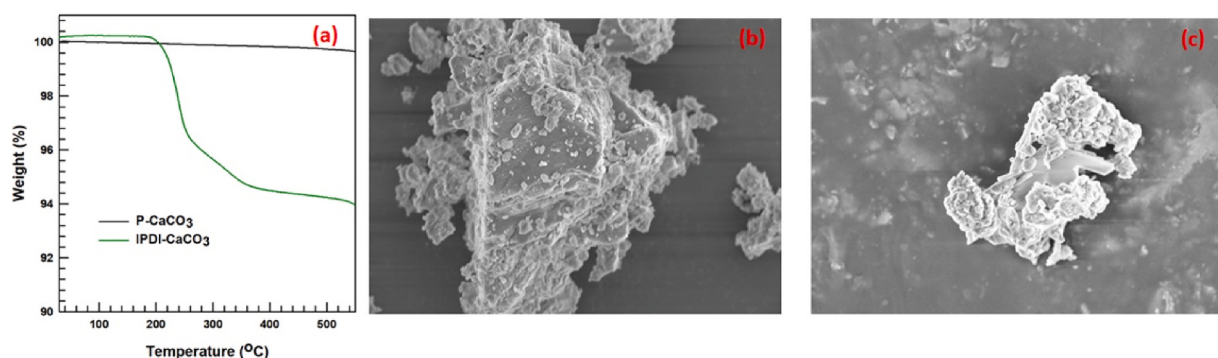


Fig. 2. Characterization of IPDI treated CaCO_3 particles: (a) thermal degradation property of the pristine and IPDI treated CaCO_3 particles; (b) and (c) the FE-SEM results of the pristine CaCO_3 and IPDI treated CaCO_3 particles respectively.

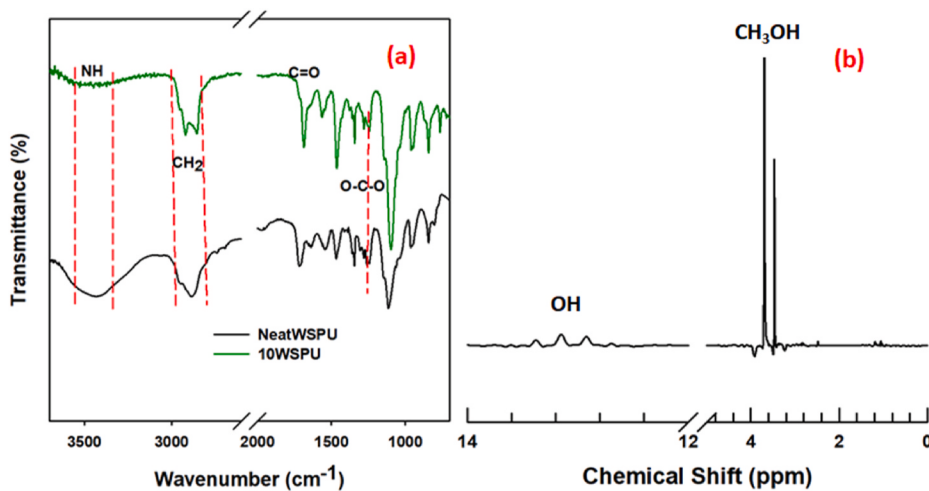


Fig. 3. Structural confirmation of the WPU: (a) FTIR analysis results; (b) HNMR.

Contact angle investigation was used to determine the hydrophilic properties of the WPU and its CaCO_3 composites. Materials with a contact angle above 90° are assumed to be highly hydrophobic, while those with a contact angle below 90° are considered hydrophilic. The results of the contact angle investigation are shown in Fig. 4 (a). The contact angles of the neat WPU and the composites exhibit insignificant

differences; however, the neat WPU is highly hydrophilic as compared to the composite. This might be due to the incorporation of CaCO_3 particles to the WPU matrix. Interestingly, the contact angle for even the 40% CaCO_3 -WPU composites is less than 65, indicating that it is highly hydrophilic. This hydrophilicity arises from the emulsifying groups and the usage of polyisocyanates which are water-soluble and hydrophilic. The

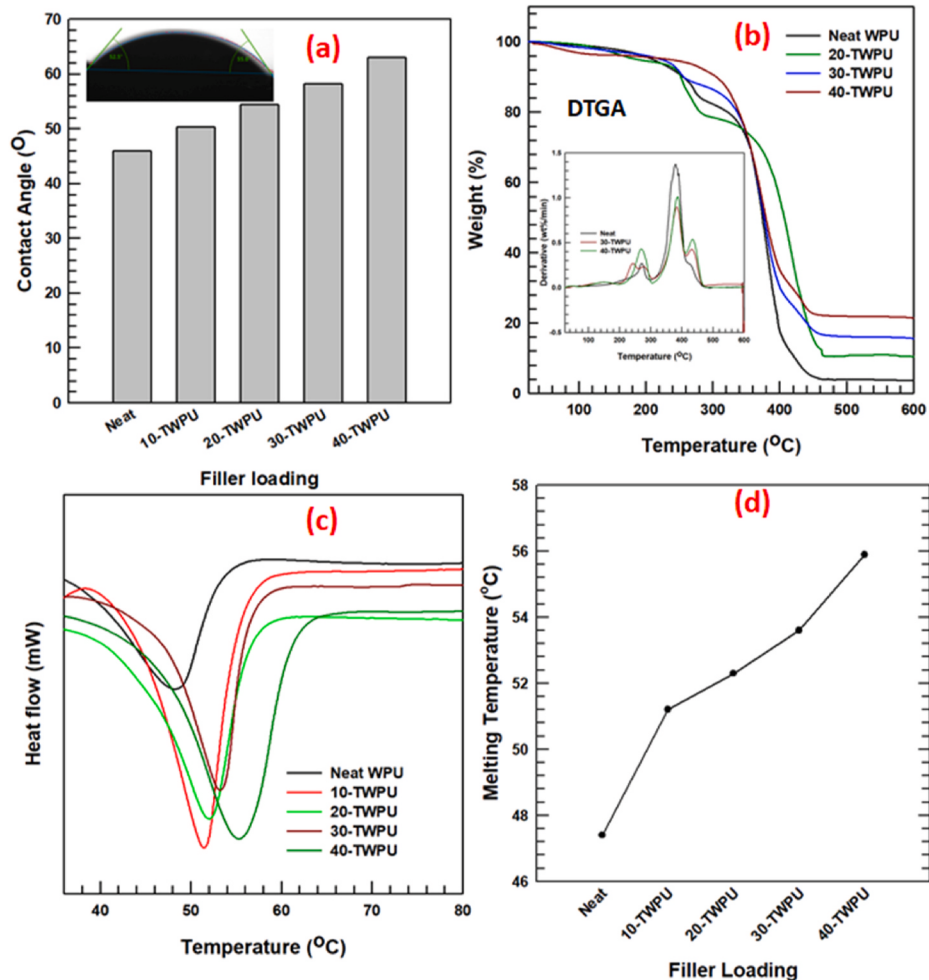


Fig. 4. Hydrophilic and thermal property: (a) contact angle measurement results; (b) Thermal degradation property of the WPU composites; (c) melting point determination with the usage of DSC; (d) Melting point changes incurred upon application of CaCO_3 particles.

contact angle measurement results were displayed in [Table 2](#).

The thermal decomposition characteristics of the WPU and WPU-CaCO₃ composites were evaluated by TGA, as shown in [Fig. 4](#) (b). Generally, increasing the IPDI-treated CaCO₃ particle weight percentage improved the thermal stability of the composites. The 40T-WPU composites were stable at temperatures up to 320 °C, whereas the neat WPU degraded at 210 °C. The neat WPU has two stages of thermal degradation; as the weight of the CaCO₃ increases, the stages tend to disappear, and the 30T-WPU composites exhibit a single-stage degradation. The initial stage of thermal degradation for the neat WPU begins around 170 °C, which is an improvement on our previous work [10] wherein the first stage of thermal degradation started at 130 °C. This stage for the neat WPU continues until the temperature reaches 320 °C, at which the second stage of thermal degradation begins and the degradation continues at an increasing rate until the temperature reaches 430 °C. Approximately 10% of the neat WPU degrades at 245 °C (T_{10%}), whereas the T_{10%} of the 40T-WPU was 305 °C. Thus, there is a 60 °C increase in the decomposition temperature for the 40T-WPU over the neat WPU. Moreover, the DTGA curves depicted the rate of thermal degradation. The results display, the rate of thermal degradation of neat WPU is higher than that of the composites; however, the maximum thermal degradation temperature has increased with increasing the loading percentage of CaCO₃ particles, it is 275 °C, 384 °C, 387 °C for the neat WPU, 30-TWPU and 40-TWSPU respectively.

The melting point is the temperature at which a substance changes from a solid state to a liquid state or the temperature at which both states survive at equilibrium. We measured the melting temperatures of our samples via DSC analysis at a heating rate of 10 °C/min at atmospheric pressure. The melting properties of WPU and its composites are shown in [Fig. 4](#) (c, d). These results show that the melting point increases slightly as the weight percentage of CaCO₃ particles increases. This might be due to high interfacial interaction between the WPU and CaCO₃ particles which in turn helps to be applied at higher temperatures. [Table 2](#) shows the respective melting points of all the specimens measured. The slight increase in the melting point occurred due to the incorporation of the CaCO₃ particles into the WPU matrix. Therefore, the use of CaCO₃ particles in an aliphatic polyisocyanate-based WPU improves the melting point of the neat WPU.

The interfacial interactions and morphological appearance of the WPU and its CaCO₃-WPU composites, evaluated using the FE-SEM spectroscopy analysis, are shown in [Fig. 5](#). The images were taken at a magnification of 1 μm. [Fig. 5](#) (a) shows the smooth surface of a fractured neat WPU. [Fig. 5](#) (b) shows the 40-WPU, which is the pristine CaCO₃ water-soluble polyurethane composite; the figure shows an aggregate that appears on the surface of the WPU matrix, which has low interfacial interactions between the CaCO₃ particles and the WPU matrix. However, as indicated in [Fig. 5](#) (c), the 40T-WPU exhibits good interfacial interactions and excellent adhesion between the CaCO₃ particles and the WPU matrix. This due to the IPDI surface treatment which acts as a compatibilizer between the polyol and the polyisocyanates.

Table 2

The thermal property and contact angle measurement results of WPU and its CaCO₃ composites.

Specimen	Melting point (°C)	Melting enthalpy (J/g. K)	On-set temperature (°C)	Off-set temperature (°C)	Contact angle (°)
Neat	47.4	42.3	45.9	55.5	45.9
10-TWPU	51.2	50.3	42.6	56.7	50.3
20-TWPU	52.3	58.3	43.02	56.4	54.4
30-TWPU	53.6	68.3	45.0	60.0	58.3
40-TWPU	55.9	79.4	43.7	58.9	63.1

Additionally, IPDI enhances the interfacial interactions as the NCO groups interact with the OH groups originating from PEG; moreover, the attachment of OH groups to the CaCO₃ particles enhances the interfacial interactions between polyisocyanate and the CaCO₃ particles.

The tensile properties, and the elongation at break of the neat WPU and its composites were evaluated using a universal testing machine (UTM) with a load of 2 KN at a rate of 10 mm/s at room temperature. The inclusion of CaCO₃ particles in the WPU significantly increased the tensile strength of the polymer, as shown in [Fig. 6](#) (a). The lowest tensile strength was observed for the neat WPU, 1.9 MPa, whereas the 40T-WPU composite exhibits the highest tensile strength, which is around 6.7 MPa. As compared to our previous report [10], we have approximately doubled the tensile strength with the same filler percentage. This is due to the usage of the polyisocyanate as the main hard segment, as in the previous study, IPDI was used as the main hard segment. The elongation at break was taken the break point. Unlike our previous works [10], which showed a decrease in the elongation at break after the inclusion of CaCO₃ particles, here, we found an increase in the elongation at break point. This might be due to the perfect incorporation of CaCO₃ particles into the WPU matrix arising from the isocyanate surface treatment which acts as a compatibilizer between the polyol and polyisocyanate. Moreover, as [Fig. 6](#) (b) indicates, the elongation at break of the 40-WPU is also greater than that of the neat WPU, which implies that the elongation at break is not dependent only on the IPDI treatment but also upon the usage of polyisocyanate as the main hard segment component in the synthesis of the polymer. Thus, using polyisocyanate as the hard segment and treating the surface of CaCO₃ with isocyanates improves the elongation at break of the composites.

The viscoelastic characteristics, the storage modulus, and tan δ were evaluated using dynamic mechanical analysis (DMA). The temperature range used to evaluate this analysis was -60 °C–65 °C at a heating rate of 10 °C/min. Pressurized liquid nitrogen was used for cooling. The results of this analysis are shown in [Fig. 6](#) (c) and (d).

The storage modulus is the reflection of the material stiffness; it dictates the stored energy of a material. A material with a higher storage modulus value is very stiff with a lot of stored energy and vice versa. We observed a huge increase in the storage modulus with the inclusion of CaCO₃ particles; the storage modulus of the 40T-WPU increased by approximately 300% as compared to the neat WPU as shown in [Fig. 6](#) (c). The glass transition region shifts to the left after the inclusion of the IPDI-treated CaCO₃ particles and slightly to the right after the inclusion of pristine CaCO₃ particles. This may be due to the treatment of the particles with IPDI. Furthermore, the 410T-WPU exhibits a 97% increase in the storage modulus compared to the same weight loading of pristine CaCO₃. The tandelta results are shown in [Fig. 6](#) (d). The wide maximum peak is taken as the glass transition temperature of the material; the figure demonstrates a T_g stabilization region around 25–32 °C. The height of the peak decreased for the IPDI-treated CaCO₃ particle composites, while the peak height increases with the inclusion of the pristine CaCO₃ particles.

5. Conclusion

Aliphatic polyisocyanate-based WPU composites of IPDI-treated CaCO₃ particles were prepared by in-situ polymerization via solution polymerization. The attachment of IPDI was confirmed via FTIR, XPS, TGA, and SEM analyses. The chemical structure of the WPU was evaluated by FTIR and NMR. The morphology was analyzed using FE-SEM spectroscopy, showing good interfacial interactions between the IPDI-treated CaCO₃ particles and the WPU matrix. The thermal stability and melting point of the fabricated WPU composites were evaluated by TGA and DSC; the results demonstrate an improvement in the thermal stability of the WPU upon the inclusion of CaCO₃ particles and a slight increase in the melting temperature. The mechanical property results demonstrate that the tensile strength and the storage modulus improved by about 3.5 times and about 300% in comparison to the neat WPU,

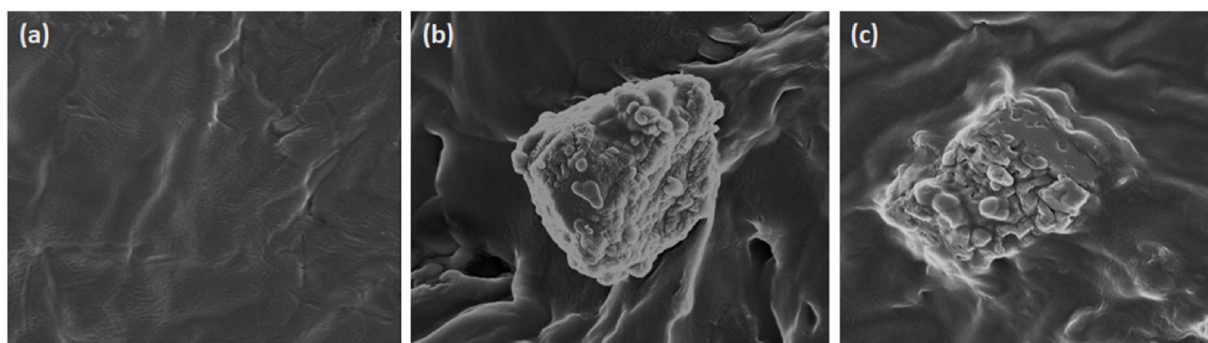


Fig. 5. Morphology analysis: (a) surface fractured neat WPU; (b) pristine CaCO_3 and WPU composites (40WPU); (c) WPU-IPDI treated CaCO_3 particles composites (40-TWPU).

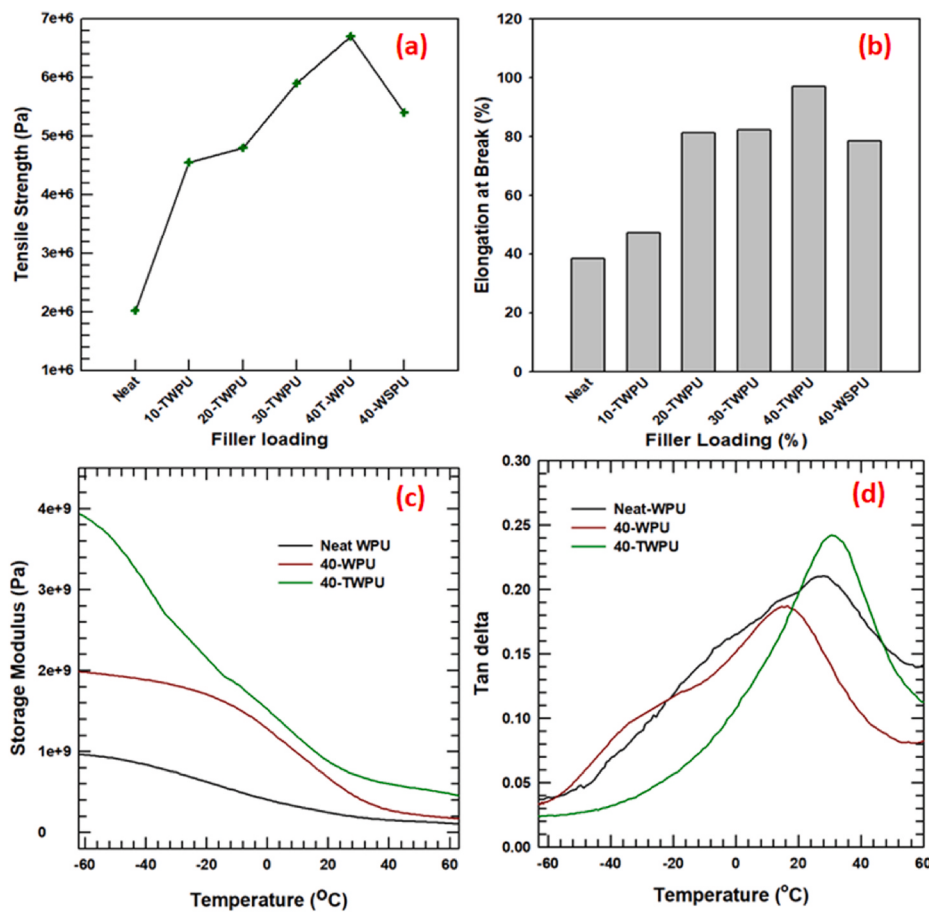


Fig. 6. Mechanical property analysis: (a) Tensile Strength (b) The elongation at break point; (c) Storage modulus; (d) $\tan\delta$ peak.

respectively.

Date availability

All data generated or analyzed during this study are included in this paper. Raw datasets are available from the corresponding author on reasonable request.

CRediT authorship contribution statement

Eyob Wondu: Conceptualization, Data curation, Formal analysis, Investigation, Writing. **Zelalem Chernet Lule:** Methodology, Visualization, Software. **Jooheon Kim:** Project administration, Supervision,

Validation.

Declaration of competing interest

The authors declare that they have no known competing financial interests or personal relationships that could have appeared to influence the work reported in this paper.

Acknowledgement

This research was supported by the MSIT (Ministry of Science and ICT), Korea, under the ITRC (Information Technology Research Center) support program supervised by the IITP (Institute of Information &

Communications Technology Planning & Evaluation) (IITP-2020-2020-0-01655).

References

- [1] S.B. Borrelle, C.M. Rochman, M. Liboiron, A.L. Bond, A. Lusher, H. Bradshaw, J. F. Provencher, Why we need an international agreement on marine plastic pollution, *Proc. Natl. Acad. Sci. U.S.A.* 114 (2017) 9994–9997, <https://doi.org/10.1073/pnas.1714450114>.
- [2] E. Wondu, Z.C. Lule, J. Kim, Fabrication of aliphatic water-soluble polyurethane composites with silane treated CaCO₃, *Polymers* 12 (2020) 747, <https://doi.org/10.3390/polym12040747>.
- [3] C.Y. Lin, K.H. Liao, C.F. Su, C.H. Kuo, K.H. Hsieh, Smart temperature-controlled water vapor permeable polyurethane film, *J. Membr. Sci.* 299 (2007) 91–96, <https://doi.org/10.1016/j.memsci.2007.04.028>.
- [4] F. Gaudin, N. Sintes-Zydowicz, Poly(urethane-urea) nanocapsules prepared by interfacial step polymerisation in miniemulsion. The droplet size: a key-factor for the molecular and thermal characteristics of the polymeric membrane of the nanocapsules? *Colloids Surf. A Physicochem. Eng. Asp.* 384 (2011) 698–712, <https://doi.org/10.1016/j.colsurfa.2011.05.050>.
- [5] K. Malkappa, T. Jana, Hydrophobic, water-dispersible polyurethane: role of polybutadiene diol structure, *Ind. Eng. Chem. Res.* 54 (2015) 7423–7435, <https://doi.org/10.1021/acs.iecr.5b01618>.
- [6] H. Sardon, L. Irusta, M.J. Fernández-Berridi, M. Lansalot, E. Bourgeat-Lami, Synthesis of room temperature self-curable waterborne hybrid polyurethanes functionalized with (3-aminopropyl)triethoxysilane (APTES), *Polymer* 51 (2010) 5051–5057, <https://doi.org/10.1016/j.polymer.2010.08.035>.
- [7] J.Y. Kwon, H. Do Kim, Preparation and properties of crosslinkable waterborne polyurethanes containing aminoplast(I), *Macromol. Res.* 14 (2006) 373–382, <https://doi.org/10.1007/BF03219097>.
- [8] H. Zhou, Y. Liu, M. Zhang, Y. Lu, L.P. Arnett, M. Soleimani, M.A. Winnik, Characterization of an aqueous dispersion of a hydrophilic polyisocyanate for waterborne two-pack polyurethane coatings, *ACS Appl. Polym. Mater.* 2 (2020) 1491–1499, <https://doi.org/10.1021/acsapm.9b01173>.
- [9] X. Gao, Y. Zhu, S. Zhou, W. Gao, Z. Wang, B. Zhou, Preparation and characterization of well-dispersed waterborne polyurethane/CaCO₃ nanocomposites, *Colloids Surf. A Physicochem. Eng. Asp.* 377 (2011) 312–317, <https://doi.org/10.1016/j.colsurfa.2011.01.025>.
- [10] E. Wondu, Z.C. Lule, J. Kim, Water-soluble polyurethane/CaCO₃ composites for gunpowder storage, *Polym. Compos.* (2020) 1–9, <https://doi.org/10.1002/pc.25736>.
- [11] A.Y. Khosrourshahi, H. Naderi-Manesh, H. Yeganeh, J. Barar, Y. Omidi, Novel water-soluble polyurethane nanomicelles for cancer chemotherapy: physicochemical characterization and cellular activities, *J. Nanobiotechnol.* 10 (2012) 1–15, <https://doi.org/10.1186/1477-3155-10-2>.
- [12] E. Wondu, H.W. Oh, J. Kim, Effect of DMPA and molecular weight of polyethylene glycol on water-soluble polyurethane, *Polymers* 11 (2019) 1915, <https://doi.org/10.3390/polym11121915>.
- [13] A.K. Nanda, D.A. Wicks, S.A. Madbouly, J.U. Otaigbe, Nanostructured polyurethane/POSS hybrid aqueous dispersions prepared by homogeneous solution polymerization, *Macromolecules* 39 (2006) 7037–7043, <https://doi.org/10.1021/ma060809h>.
- [14] M.M. Rahman, H. Zahir, H. Do Kim, Synthesis and properties of waterborne polyurethane (WBU)/modified lignin amine (MLA) adhesive: a promising adhesive material, *Polymers* 8 (2016), <https://doi.org/10.3390/polym8090318>.
- [15] X. Yin, Y. Luo, J. Zhang, Synthesis and characterization of halogen-free flame retardant two-component waterborne polyurethane by different modification, *Ind. Eng. Chem. Res.* 56 (2017) 1791–1802, <https://doi.org/10.1021/acs.iecr.6b04452>.
- [16] H. Zhu, S.A. Xu, Preparation and fire behavior of rigid polyurethane foams synthesized from modified urea-melamine-formaldehyde resins, *RSC Adv.* 8 (2018) 17879–17887, <https://doi.org/10.1039/c8ra01846d>.
- [17] R.A. Chowdhury, C.M. Clarkson, S. Shrestha, S.M. El Awad Azrak, M. Mavlan, J. P. Youngblood, High-performance waterborne polyurethane coating based on a blocked isocyanate with cellulose nanocrystals (CNC) as the polyol, *ACS Appl. Polym. Mater.* 2 (2020) 385–393, <https://doi.org/10.1021/acspolym.9b00849>.
- [18] J. Zhao, W. Zhu, X. Wang, L. Liu, J. Yu, B. Ding, Fluorine-Free waterborne coating for environmentally friendly, robustly water-resistant, and highly breathable fibrous textiles, *ACS Nano* 14 (2020) 1045–1054, <https://doi.org/10.1021/acsnano.9b08595>.
- [19] I. Díez-García, A. Santamaría-Echart, A. Eceiza, A. Tercjak, Triblock copolymers containing hydrophilic PEO blocks as effective polyols for organic solvent-free waterborne poly(urethane-urea)s, *React. Funct. Polym.* 131 (2018) 1–11, <https://doi.org/10.1016/j.reactfunctpolym.2018.07.003>.
- [20] P.D. Michael Szycher, Szycher's handbook of polyurethanes, *Choice Rev. Online*. 37 (1999), <https://doi.org/10.5860/choice.37-1570>, 37-1570–37-1570.
- [21] X. Wang, W. Xing, L. Song, H. Yang, Y. Hu, G.H. Yeoh, Fabrication and characterization of graphene-reinforced waterborne polyurethane nanocomposite coatings by the sol-gel method, *Surf. Coating. Technol.* 206 (2012) 4778–4784, <https://doi.org/10.1016/j.surcoat.2012.03.077>.
- [22] X. Zhou, Y. Li, C. Fang, S. Li, Y. Cheng, W. Lei, X. Meng, Recent advances in synthesis of waterborne polyurethane and their application in water-based ink: a review, *J. Mater. Sci. Technol.* 31 (2015) 708–722, <https://doi.org/10.1016/j.jmst.2015.03.002>.
- [23] Z. Wu, H. Wang, M. Xue, X. Tian, H. Zhou, X. Ye, K. Zheng, Z. Cui, Preparation of carbon nanotubes/waterborne polyurethane composites with the emulsion particles assisted dispersion of carbon nanotubes, *Compos. Sci. Technol.* 114 (2015) 50–56, <https://doi.org/10.1016/j.compscitech.2015.02.020>.
- [24] H.T. Lee, L.H. Lin, Waterborne polyurethane/clay nanocomposites: novel effects of the clay and its interlayer ions on the morphology and physical and electrical properties, *Macromolecules* 39 (2006) 6133–6141, <https://doi.org/10.1021/ma060621y>.
- [25] B.K. Kim, Aqueous polyurethane dispersions, *Colloid Polym. Sci.* 274 (1996) 599–611, <https://doi.org/10.1007/BF00653056>.
- [26] H. Honarkar, Waterborne polyurethanes: a review, *J. Dispersion Sci. Technol.* 39 (2018) 507–516, <https://doi.org/10.1080/01932691.2017.1327818>.
- [27] L. Lei, L. Zhong, X. Lin, Y. Li, Z. Xia, Synthesis and characterization of waterborne polyurethane dispersions with different chain extenders for potential application in waterborne ink, *Chem. Eng. J.* 253 (2014) 518–525, <https://doi.org/10.1016/j.cej.2014.05.044>.
- [28] H.C. Kuan, H.Y. Su, C.C.M. Ma, Synthesis and characterization of polysilicic acid nanoparticles/waterborne polyurethane nanocomposite, *J. Mater. Sci.* 40 (2005) 6063–6070, <https://doi.org/10.1007/s10853-005-1302-7>.
- [29] M. Szycher, in: second ed. Health and Safety, Szychers Handb. Polyurethanes, vol. 32, 2012, <https://doi.org/10.1201/b12343>, 449–494.
- [30] G. Wypych, in: 2016th ed. Handbook of Polymers 2nd Edition George Wypych, ChemTech Publishing, Toronto, 2016. http://www.manaepd.com/images/handbook_of_polymer.pdf.